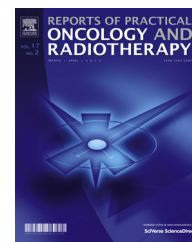


Available online at www.sciencedirect.com

ScienceDirect

journal homepage: <http://www.elsevier.com/locate/rpor>

Original research article

Study of gold nanoparticles for mammography diagnostic and radiotherapy improvements[☆]

Lorenzo Torrissi^{a,*}, Nancy Restuccia^a, Alfio Torrissi^b^a Dipartimento di Scienze Matematiche e Informatiche, Scienze Fisiche e Scienze della Terra, V.le F.S. d'Alcontres 31, 98166 S. Agata, Messina, Italy^b Nuclear Physics Institute, CAS, 25068 Rez, Czech Republic

ARTICLE INFO

Article history:

Received 29 December 2018

Received in revised form

23 April 2019

Accepted 10 July 2019

Available online 30 July 2019

Keywords:

Gold nanoparticles

Mammography

Diagnostics

Radiotherapy

ABSTRACT

Aim: A study on the possibility to use gold nanoparticles in mammography, both for a better image diagnostics and radiotherapy, is presented and discussed. We evaluate quantitatively the increment of dose released to the tumor enriched with Au-NPs with respect to the near healthy tissues, finding that for X-rays the increase can reach two orders of greater intensity. **Background:** Gold nanoparticles continue to be investigated for their potential to improve existing therapies and to develop novel therapies. They are simple to obtain, can be functionalized with different chemical approaches, are stable, non-toxic, non-immunogenic and have high permeability and retention effects in the tumor cells. The possibility to use these for breast calcified tumors to be better treated by radiotherapy is presented as a possible method to destroy the tumor.

Materials and methods: The nanoparticles can be generated in water using the top-down method, should have a size of the order of 10–20 nm and be treated to avoid their coalescence. Under diagnostic X-ray monitoring, the solution containing nanoparticles can be injected locally inside the tumor site avoiding injection in healthy tissues. The concentrations that can be used should be of the order of 10 mg/ml or higher.

Results: An enhancement of the computerized tomography diagnostics using 80–150 keV energy is expected, due to the higher mass X-ray coefficient attenuation with respect to other contrast media. Due to the increment of the effective atomic number of the biological tissue containing the gold nanoparticles, also an improvement of the radiotherapy effect using about 30 keV X-ray energy is expected, due to the higher photoelectric cross sections involved.

Conclusions: The study carried out represents a feasibility proposal for the use of Au-nanoparticles for mammographic molecular imaging aimed at radiotherapy of tumor nodules but no clinical results are presented.

© 2019 Greater Poland Cancer Centre. Published by Elsevier B.V. All rights reserved.

[☆] Article from the Special Issue on Nanoparticle and Immunotherapy.

* Corresponding author.

E-mail address: lorenzo.torrissi@unime.it (L. Torrissi).<https://doi.org/10.1016/j.rpor.2019.07.005>

1507-1367/© 2019 Greater Poland Cancer Centre. Published by Elsevier B.V. All rights reserved.

1. Background

Gold nanoparticles (Au-NPs) can be used to increase the contrast of bio-medical images and their spatial resolution.¹ In particular, they are expected to be used in mammography for the observation of mammary tumor nodules. The presence of gold, uniformly distributed in the tumor site of the breast, increases the effective atomic number Z_{eff} of the tissue and permits to enhance significantly the contrast as it increases the photoelectric effect cross-section σ_p , depending strongly on the atomic number according to the relation²:

$$\sigma_p = \text{constant} \cdot \frac{Z_{\text{eff}}^n}{E^3}, \quad (1)$$

where E is photon energy and n is an exponent which varies between 4 and 5.

The Murthy³ proposed formula for the effective atomic number, Z_{eff} is the following:

$$Z_{\text{eff}} = \sqrt[2.94]{f_1 \cdot (Z_1)^{2.94} + f_2 \cdot (Z_2)^{2.94} + f_3 \cdot (Z_3)^{2.94} + \dots}, \quad (2)$$

where f_n is the fraction of the total number of electrons associated with each element, and Z_n is the atomic number of each element.

At the low energy used for mammographic X-ray images energies (~20–30 keV), Au-NPs show exceptionally attenuation even at very low concentration levels. The use of such contrast agents allows high-resolution imaging *in vivo* and permits to be employed as the targeting of the tumor tissues in case of radiotherapy.

The dose released by radiotherapy using X-rays and other ionizing radiations can be increased for the enhancement of the mass attenuation coefficient or for the particle stopping powers in the tissues containing Au-NPs.

In order to improve their stability in biological solutions, the AuNP can be conjugated to polyethylene glycol (PEG) peptides.⁴ In addition, Au-NPs can be functionalized with different groups (amine, carboxyl, peptide, DNA, RNA, antibodies) to be able to carry out specific actions, such as adherence to the cell membrane, RNA carrier, targeting carcinoma cells, and others.⁴

In this ambit, special attention is devoted to the admission of Au-NPs in the tumor tissue. More techniques of Au-NPs admission to the tumor cells can be employed. The liquid solution can be added by mechanical injection in the tumor site, using a method of distribution as uniform as possible and avoiding injection in the near healthy tissues. It can be transported via blood flux by injecting the solution containing Au-NPs in the blood vessels or by spraying the breast tissue, with special regard to those spraying the highly branched tumor tissue.⁵ It can be transported using functionalized Au-NPs with specific molecules adapted to be better accepted by the specific tumor tissue. For example, Au-NPs can be functionalized with PEG (polyethylene glycol) which improves the *in vivo* stability, avoiding uptake by the reticular endothelial system, or with affibody molecules, which are small, robust proteins, of the antibody family.⁶ Peptides and proteins may represent promising tools to improve the delivery of AuNPs to

cancer tissues. When NPs are injected intravenously, they circulate throughout the entire body. NPs escape the circulatory system to other tissues by endocytosis, shear forces, or passive diffusion through fenestrations in the capillary network. Generally, NPs less than 6 nm are largely cleared by the kidney, whereas those larger than 6 nm are cleared by the liver. The biodistribution of the gold nanoparticles depends strongly on the type of functionalized nanoparticles and on the modality of injection in the tumor tissues.

Au-NPs can be also bonded to specific phages, such as the M13, which permit the transport to specific cancer cells, to cross their membrane thickness and to release the Au-NP near cell nucleus, targeting the DNA with a spatial localization.⁷

2. Aim

The introduction of Au-NPs in the tumor site can be observed using X-ray absorption or by a secondary fluorescence emission of the gold particles, permitting a contrast image compared to the surrounding tissues.

The use of these metallic nanoparticles arriving at the tumor tissues must be exploited immediately after the tissues are irradiated with ionizing radiations (X-rays, electrons, and ions) to enhance the dose to the tumor cells with respect to the healthy one. Also, the hyperthermia technique can be employed to enhance the temperature of the zone where the metallic nanoparticles are localized by using visible radiation at the wavelength at which surface plasmon resonance (SPR) absorption is induced.

This paper intends to present a feasibility study for the use of Au-NPs in solution to be injected into breast cancer tissues to improve CT contrast images and for potential efficiency of radiotherapy treatments. It does not present clinical results of this technique used on humans.

A study on mammary carcinoma in mice is presented to show the significant regression when submitted to Au-NPs injection and radiotherapy treatment.

3. Materials and methods

The production of Au-NPs using the so-called top-down method is performed using an Nd:YAG laser irradiating a pure Au target placed in water. The laser wavelength of 1064 nm and 532 nm, 3 ns pulse duration, 100 mJ pulse energy, 10 Hz repetition rate, and laser fluence within 5 and 30 J/cm², can be employed to realize laser ablation of gold. The gold is submerged by 10 mm of distilled water, in a glass tube with about 20 ml water. The laser beam is deflected vertically by a prism and focalized on the Au target. Generally, the spot size is circular with 0.5 mm² area, corresponding to a fluence of 20 J/cm². During the repetition rate irradiation, the target is moved not to ablate the same area and not to destroy the focal conditions.

A solution of sodium citrate was added to the Au-NPs solution as a capping, in order to avoid the NP coalescence.

Au-NPs were observed with SEM and TEM microscopy and evaluated in composition by using the characteristic X-ray fluorescence emission induced by electron beam (EDX analysis).

A mammogram using low-energy X-rays tube with a Mo anode (K-shell X-ray energies of 17.5 and 19.6 keV) is employed

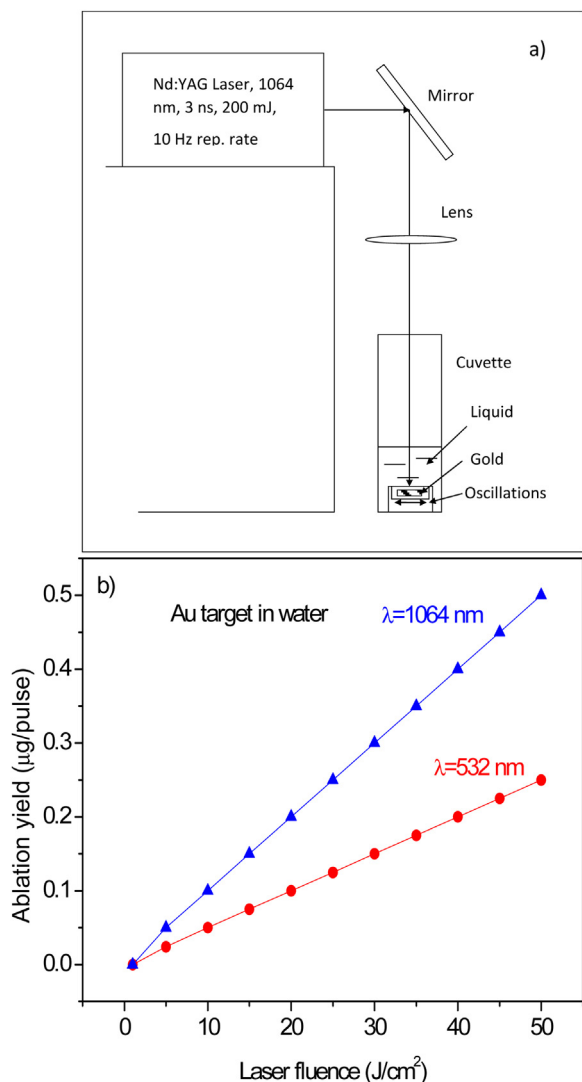


Fig. 1 – Scheme of the experimental set up used for Au-NPs production by laser (a) and ablation yield in water versus laser fluence for two wavelengths: 1064 nm and 532 nm (b).

for breast analysis at Messina University (Italy). It is a Siemens analogical mammography with 0.03 mm Mo filtration using an X-ray tube currents of 100 mA, and exposure times of 1 second or more depending on the thickness of the compressed breast. The breast images were acquired by a patient of 60 years showing filamentous microcalcifications.

NIST database⁸ was employed for the evaluation of the mass absorption coefficient in different materials and compounds. Ziegler SRIM and SREM codes^{9,10} were used for simulation of ions and electrons in matter, respectively, and for the evaluation of the particle ranges, stopping powers and straggling.

4. Results

Fig. 1a reports a typical scheme of the experimental set-up, while Fig. 1b shows the laser ablation yield, in terms of removed mass per laser shot, versus the laser fluence. It is

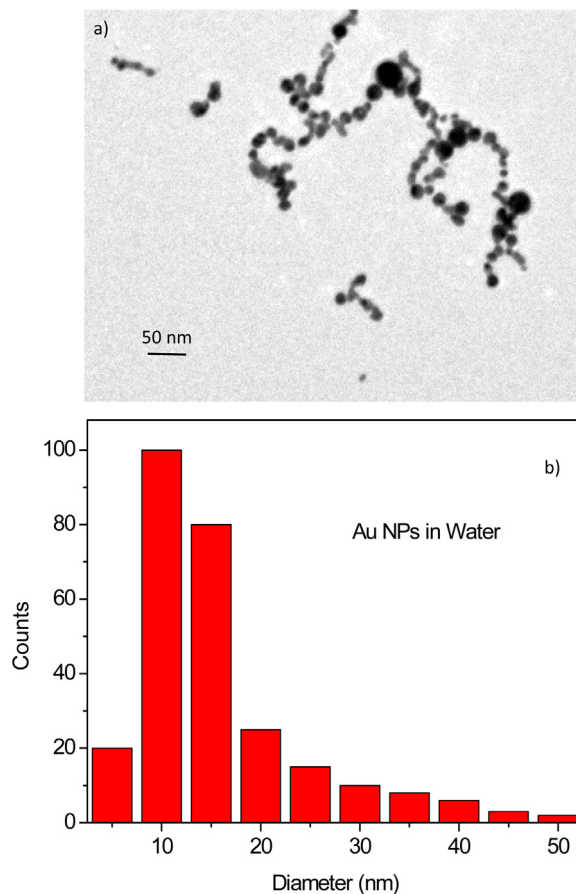


Fig. 2 – TEM image of the Au-NPs produced in water (a) and histogram of the nanoparticle diameter distribution (b).

possible to observe that using 20 J/cm^2 fluence and 532 nm wavelength, the ablation yield in water is about $0.1\ \mu\text{g/pulse}$.

Plasma produced at the solid-liquid interface generates a bubble of ionized gas, which expands up to implode due to the liquid confinement, generating atoms nucleation, quenching and nanoparticles production in water suspension. In order to avoid nanoparticles coalescence, sodium citrate was added to the Au-NPs solution at a minimum concentration of $1\ \mu\text{g/ml}$. Such cupping compound creates a thin layer around the negatively charged nanoparticles, which tends to hinder their approach by a repulsive Coulombian effect.

The TEM analysis of nanoparticles has permitted to evaluate the shape and the size of the nanoparticles and the dimension of little aggregated. The NP shape was spherical and the average diameter was about 10–15 nm. Fig. 2a shows a typical image of the nanoparticles observed at TEM microscopy. EDX analysis has demonstrated that the NPs are of pure gold.

A traditional mammogram was employed to obtain images of a healthy and diseased breast by using low-energy X-rays tube with a Mo anode (K-shell X-ray energies of 17.5 and 19.6 keV). A typical image of a healthy breast is reported in Fig. 3a indicating a uniform X-ray absorption of the tissues.

Fig. 3b reports on a breast with an apical conical tumor observable from the density increment on these diseased tissues (whiter color on the X-ray mammography). A cone with

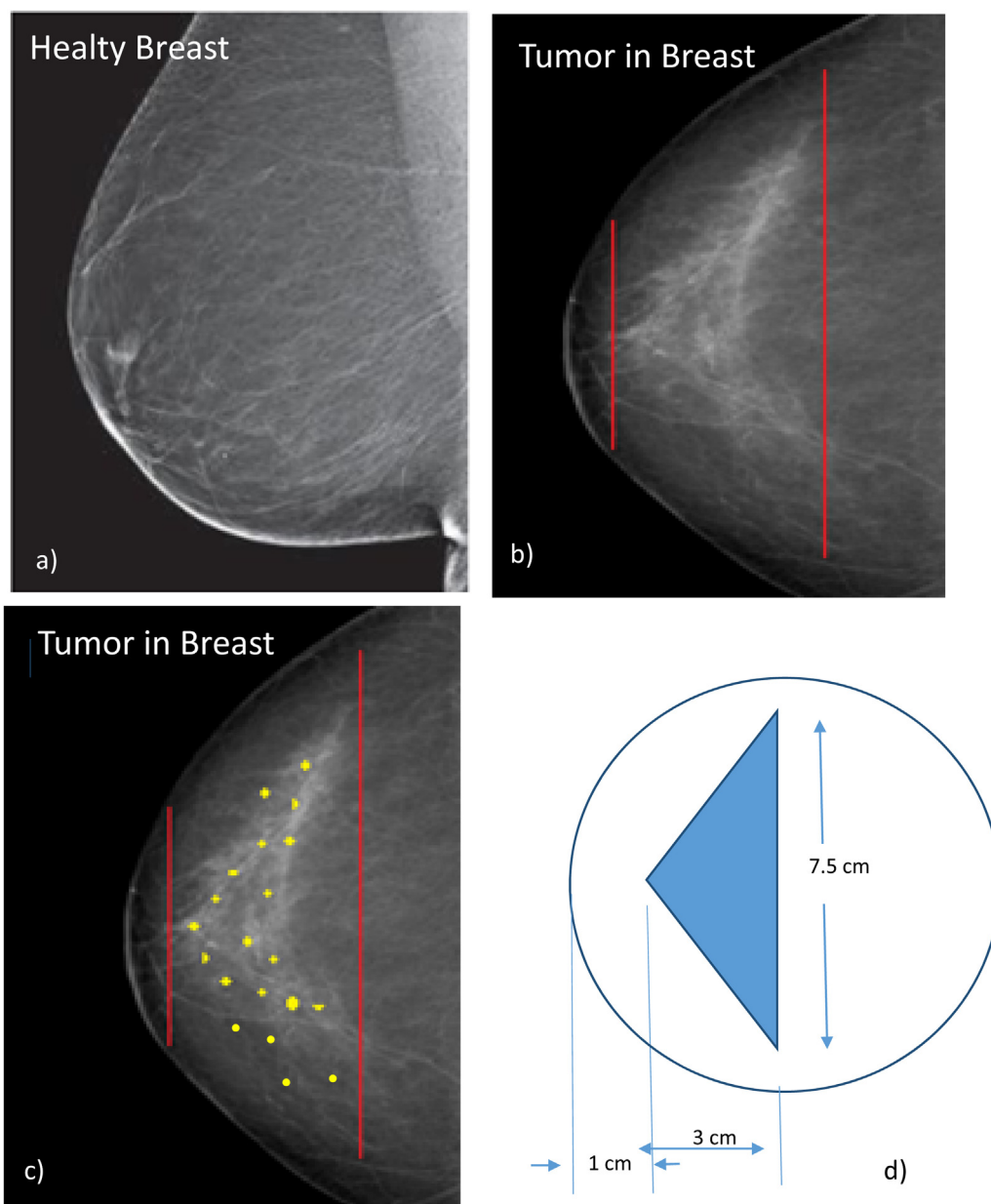


Fig. 3 – Mammogram image of the healthy breast (a), the breast with calcified tumor (b), the image schematizes the insertion of Au-NPs in the tumor tissue (c) and the geometrical dimension of the tumor volume (d).

3 cm height and 7.5 cm base diameter represents the dimension of these calcium densified tumor tissues.¹¹

The tumor is located at the depth of 1 cm in the breast and has 3 cm in thickness; around it, healthy tissue is present. Thus, for efficient radiotherapy applications, it is necessary to consider the healthy tissue around the tumor to minimize the dose released to it and maximize the dose released to the tumor nodule. In this optic, Au-NPs could be injected locally in the conical tumor, as represented in Fig. 3c by the yellow points indicating an approximated uniform distribution. The improvement of the radiotherapy efficiency will be evaluated by the real dose released to the surface of the healthy tissue with respect to that released in the tumor site by using Au-NPs with respect to the case without them.

In order to introduce the advantage of Au-NPs use in diagnostics, Fig. 4 reports the comparison of the attenuation coefficients versus X-ray energy for soft tissue (breast), bone and gold, and for two contrast media: iodine and gadolinium.¹² It is possible to observe that the lower mass attenuation coefficient is found for the healthy soft tissue, while the higher, for gold, followed by gadolinium and iodine. Another very commonly used contrast medium is BaSO₄ with absorption similar to that of iodine. The absorption edges of these elements indicate that gold is the best to be used at about 20 keV energy, typical for mammography contrast imaging. Moreover, gold has a higher mass attenuation also for X-ray energy ranging between 80 and 150 keV, typical for TC diagnostic images. Furthermore, the use of stable and biocompatible

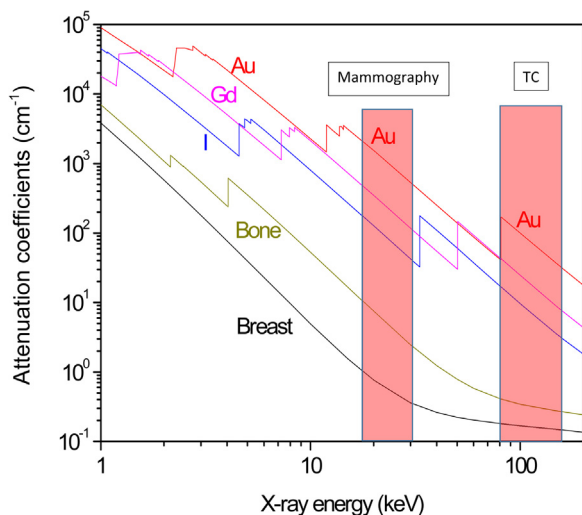


Fig. 4 – Mass attenuation coefficients versus X-ray energy for breast, bone, and different contrast medium (I, Gd and Au).

gold as nanoparticles embedded in biological tissues permits the observation of the stimulated characteristic X-ray fluorescence, generating Au X-ray imaging with high contrast and spatial resolution.

With regard to radiotherapy, breast cancer can be treated using X-rays, electron and ion beams. To this, optimum energy for X-ray irradiations is of about 100 keV, while for electrons and ions it depends on the tumor thickness, shape, position from the surface and maximum depth. For example, in the investigated case at which the tumor extends from a minimum depth of 1 cm up to a maximum depth of 4 cm, the minimum and maximum energy of the modulated electron beam, using the projected ranges, should vary between 2 and 8 MeV, respectively. In the same case, by using proton beams, the Bragg peak should be shifted between 35 and 70 MeV using the spread-out Bragg peak (SOBP) procedure,¹³ in agreement with the NIST projected range database. Of course, in all the radiotherapy treatments an adapt collimator and absorber must be employed for the irradiation in order to maximize the dose to the tumor and minimize that released to the surrounding healthy tissues.

For radiotherapy applications, one has to consider the mass attenuation coefficients and the stopping powers in the biological tissues containing a known concentration of Au-NPs. To this, we use the Bragg's rule that evaluates the mass absorption coefficient or the stopping power by the linear combination of the individual atomic elements in the compound. For the A + B compound, the ε_{A+B} stopping power or absorption coefficient can be determined by the Bragg's rule¹⁴:

$$\varepsilon_{A+B} = \frac{A}{A+B} \varepsilon_A + \frac{B}{A+B} \varepsilon_B, \quad (3)$$

where ε_A is the stopping power or absorption coefficient for X-ray, of the element A (breast tissue) of the considered compound and ε_B is the stopping power, or absorption coefficient for X-ray, of the element B (Au-NPs).

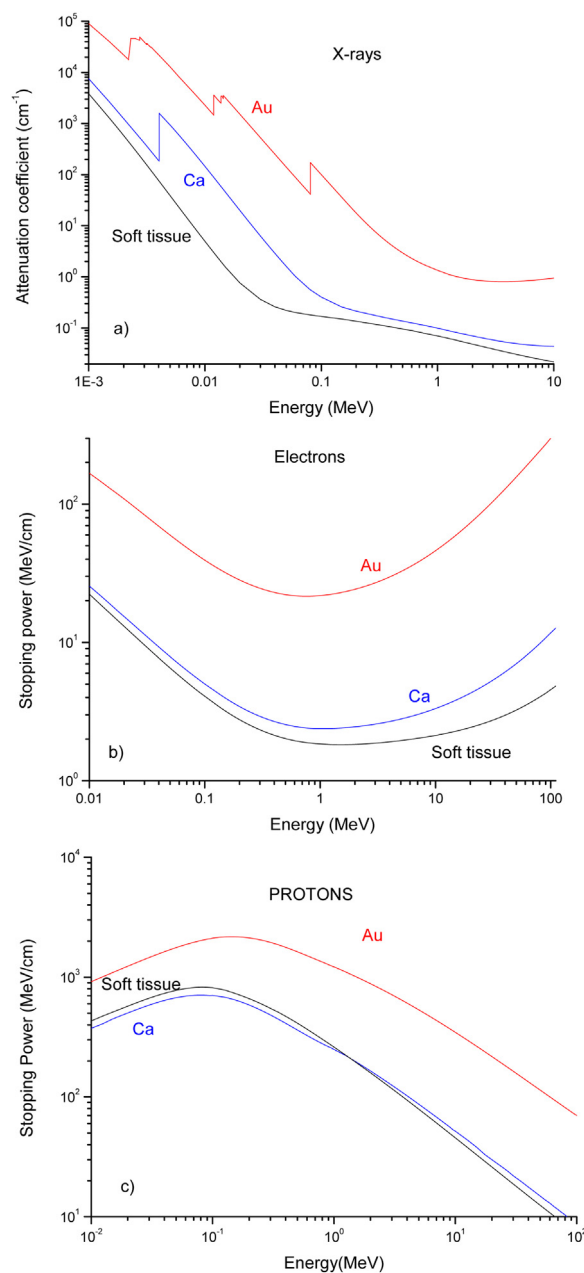


Fig. 5 – Mass attenuation coefficient (a), electron stopping power (b) and proton stopping power (c) versus the radiation energy in soft tissue (breast), Ca and Au.

Fig. 5 reports the attenuation coefficients for photons (a), and the stopping powers for electrons (b) and protons (c) relative to the soft tissue (breast), calcium (for the calcified tumor) and gold (for the presence of Au-NPs). The breast tissue is generally associated with the presence of calcified components with a mass concentration in the order of 1–10% or more; Au-NPs generally could be employed at a concentration in the order of 1–30 mg/ml. Such effects of calcification and the presence of gold nanoparticles increase the mass density, the effective atomic number, and the absorption coefficient and stopping powers of the tissue.

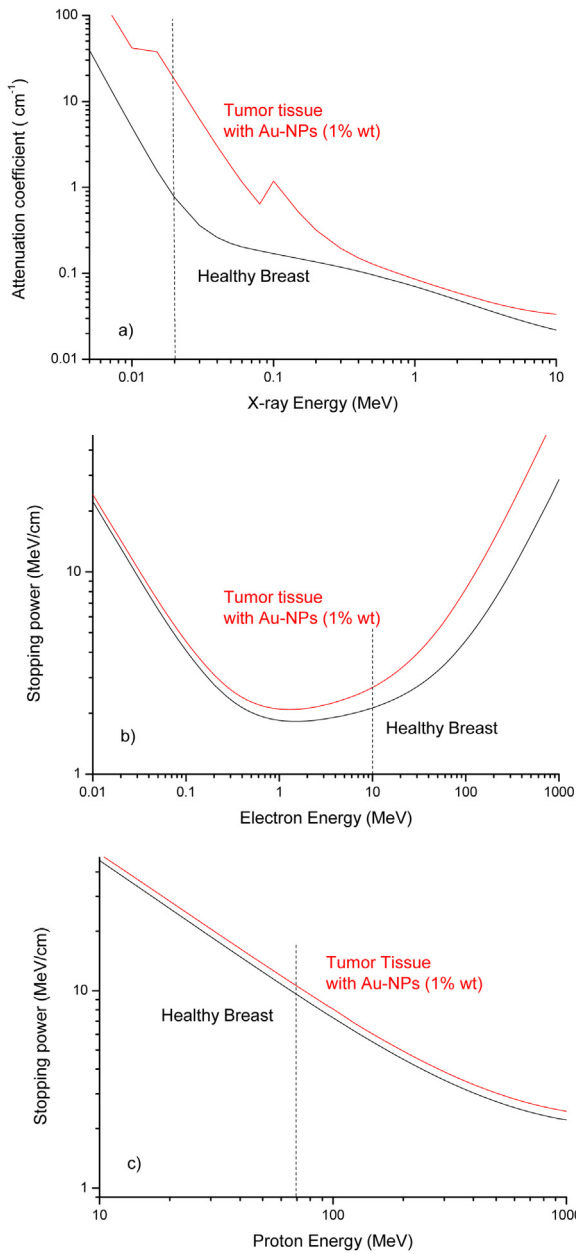


Fig. 6 – Comparison between the mass attenuation coefficient (a) and the electron (b) and proton (c) stopping powers versus the radiation energy for healthy breast tissue and tumor tissue containing 10 mg/ml Au nanoparticles.

Assuming a Ca weight concentration of 10% and an Au-NPs concentration of 10 mg/ml, i.e. this last of 1% in weight, by using the Bragg law reported in Eq. (3), it is possible to evaluate the corresponding attenuation coefficient and stopping powers of the final treated tissue, prepared with Au-NPs as a target for radiotherapy applications. Fig. 6 reports the attenuation coefficients and the stopping powers for X-rays (a), electron (b) and proton (c) beams relative to the comparison between the healthy breast tissue and the tumor tissue in which Ca and Au-NPs are enclosed. It is possible to evince from Fig. 6a that, for example, by using for radiotherapy X-ray beams at 20 keV the dose released to the tumor (proportional to the attenuation

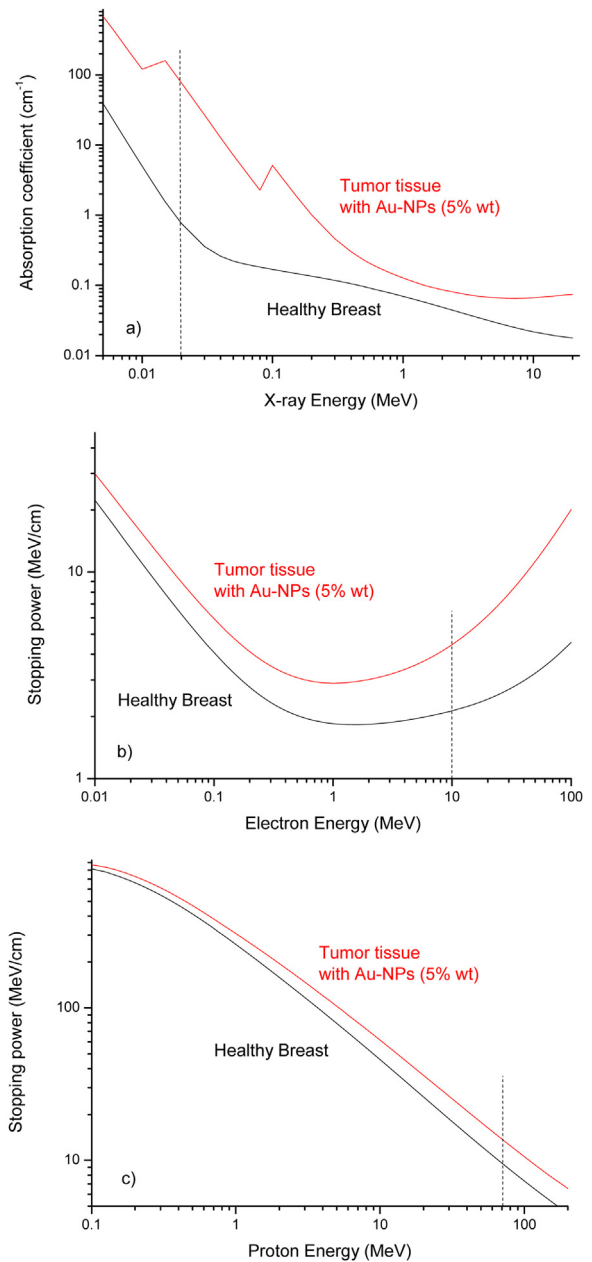


Fig. 7 – Mass attenuation coefficients (a) and electron stopping power (b) versus energy for healthy breast and tumor tissue containing different concentrations of Au-NPs.

coefficient) with respect to the healthy tissue increases significantly by a factor $R_X = 24$. This increment ratio for 10 MeV electron beam assumes the value $R_e = 1.3$, as observable from the plot of Fig. 6b. The increment is reduced only to $R_p = 1.11$ for 70 MeV protons treatment.

Thus, the improvement is well representative for low energy X-rays at which photoelectric effect promotes exponentially the interaction with high Z elements and less representative for the stopping powers of electron and proton beams. These results can be used with success both to increase the X-ray diagnostics in mammography and for classical X-ray radiotherapy of the breast.

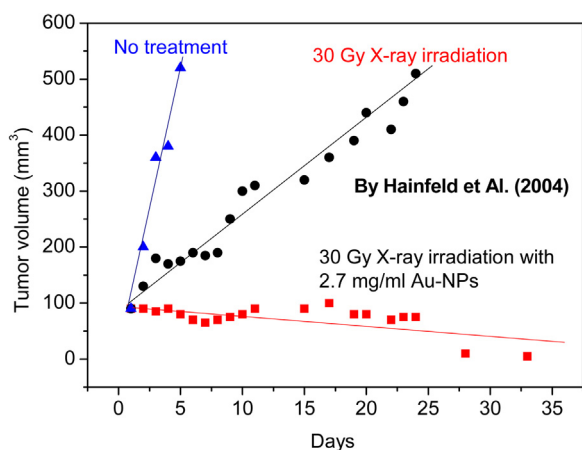


Fig. 8 – Tumor volume of mammary carcinomas in mice versus days without treatment, with simple X-ray radiotherapy treatment, and with radiotherapy treatment in the case of Au-NPs administration to the tumor tissues.¹⁴

Of course, by increasing the Au-NPs concentration the effect of the released dose is enhanced significantly, for example, by using an Au-NPs concentration 5 times higher (50 mg/ml) and 20 keV X-rays energy, as reported in Fig. 7a, the increment factor enhances up to $R_x = 110$, i.e. by about two orders of magnitude higher. For 10 MeV electrons the increment obtained the 50 mg/ml Au-NPs concentration increases up to $R_e = 2.1$, as reported in Fig. 7b. For proton therapy, by using 70 MeV protons, the increment reaches only $R_p = 1.5$.

For protons, the increment is more limited than for electrons and photons because we are using the effect of the Bragg peak at which the dose is maximized due to collisional nuclear stopping power and is not very much affected by the presence of high Au-NPs concentration.

5. Conclusions

The paper presents a study on the possibility to use Au-NPs to improve the efficiency of breast tumors. It does not report clinical results on humans because, although Au-NPs are non-toxic and non-immunogenic and have high permeability and retention effects in tumor cells, further investigation needs to be conducted before being applied to humans. A number of individual studies must be carried out on cytotoxicity, effect of NPs size on toxicity, efficacy, biodistribution, retention time, collateral effects, and physiological response of Au-NPs to human breast, which actually are under investigation for *in vitro* studies.¹⁵

The X-ray radiotherapy represents the most common treatment for a number of cancers with high effectiveness but their radio-treatment involves not only tumor tissues but also healthy ones, which receive high doses with high risks of damage and collateral risks. Radiotherapy can be optimized in order to reduce the side effects and increase the survival of cells in healthy tissue. An efficient method to reach this is to introduce into Au-NPs the tumor cells, i.e. particles with high atomic number, biocompatible, stable, which permit the

release of high doses due to their enhancement of the electron density in the target.

Although numerous studies on the size, shape, capping agent and molecular functionalization of Au-NPs have been and continue to be performed, it is still not clear enough what the optimal conditions are for the highest targeting efficiency rate of cancerous cells. Therefore, much more research work in this field is required from biologists, biochemists, chemists, pharmacologists, physicists, and doctors.

In this paper, we assume that a process of introduction of Au-NPs (functionalized or less) occurs in the tumor tissues, and we evaluate quantitatively the increment of dose released to the tumor with respect to the near healthy tissues, finding that the increase can reach two orders of greater intensity.

The result is of special interest for breast tumors, concerning a sensitive organ, which must be treated with attention by reducing as much as possible the dose to the surrounding healthy zones and enhancing that released to the treated tumors. Actually, it is not possible to proceed on humans, but promising results have been obtained *in vivo* in mice.

Hainfeld et al.¹⁶ have used mice bearing subcutaneous EMT-6 mammary carcinomas to inject intravenous 1.9 nm diameter gold particles up to 2.7 g Au/kg body weight. After the Au-NPs injection, the tumor region was irradiated with 250 kVp X-rays. The rate of tumor growth was dramatically different in mice receiving only radiation and those receiving gold nanoparticles followed by radiation. One month after mice received 30 Gy only X-ray therapy, all tumors grew about five times bigger than their initial sizes. The tumors in which Au-NPs were injected and which were subsequently irradiated with X-rays with 30 Gy dose, instead, were no longer visible, indicating that the higher released dose damaged the tumor tissues causing the tumor to regress to negligible volumes, as reported in the plot of Fig. 8.

The dose enhancement is optimal in the photoelectric-dominated X-ray spectrum, taking in consideration that the gold K-edge is at 80.7 keV. Higher photon energies reach deeper tumors but are less efficacious for the reduced ionization cross-sections and for their energy release also in the nearest healthy tissues behind and in front of the tumor site. The direct intratumoral injection of diffusible gold may also be explored. A second-generation Au-NPs agent will have a targeting molecule, such as an antibody, chemically attached to further improve tumor specificity.

Less evident but sometimes more effective in radiotherapy, seem to be electron and proton beams, which added to the stopping power increment in the presence of Au-NPs have the advantage of being fully stopped at their range, which can be controlled by their maximum energy without causing damage in the healthy tissues downstream the tumor site.

In conclusion, although the problem to insert Au-NPs in cancer cells must be further investigated and nanoparticles should be functionalized to be better transported to specific cells, the initial study of the increment of the effective atomic number of the treated tissues indicates that the dose released during diagnostics and/or radiotherapy can be significantly enhanced. A clear and optimal enhancement can be obtained using X-ray doses at energies below 80 keV, at which the photoelectric effect can be maximized and the

mammography diagnostics and breast treatment can benefit from it.

Conflict of interest

The authors declare no conflict of interest.

Financial disclosure

Authors declare that this manuscript was prepared thank to the funds of Messina University (Italy) on the base of the Project “Research and Mobility” Coordinated by Prof. L. Torrissi, Project n. 74893496.

Acknowledgements

This work was supported by the Messina University, project ‘Research and Mobility’, Grant No. 74893496.

REFERENCES

- Restuccia N, Torrissi L. Nanoparticles in liquids generated laser as contrast medium and radiotherapy intensifiers. *EPJ Web Conf* 2018;167:04007, <http://dx.doi.org/10.1051/epjconf/201816704007>.
- Turner JE. *Atoms, Radiation, and Radiation protection, II Edition*. New York: Wiley Interscience Publication; 1995. ISBN: 0471-59581-0. <http://www.nuclear.dababneh.com/Radiation-Undergrad-2/Atoms,%20Radiation,%20and%20Radiation%20Protection.pdf>.
- Murty RC. Effective atomic numbers of heterogeneous materials. *Nature* 1965;207:398–9, <http://dx.doi.org/10.1038/207398a0>.
- Tiwari PM, Vig K, Dennis VA, Singh SR. Functionalized gold nanoparticles and their biomedical applications. *Nanomaterials (Basel)* 2011;1(1):31–63.
- Torrissi L, Restuccia N, Cuzzocrea S, Paterniti I, Ielo I, Pergolizzi S, Cutroneo M, Kovacik L. Laser-produced Au nanoparticles as X-ray contrast agents for diagnostic imaging. *Gold Bull* 2017;50(1):51–60, <http://dx.doi.org/10.1007/s13404-017-0195-y>.
- Spadavecchia J, Movia D, Moore C, et al. Targeted polyethylene glycol gold nanoparticles for the treatment of pancreatic cancer: from synthesis to proof-of-concept in vitro studies. *Int J Nanomed* 2016;11:791–822, <http://dx.doi.org/10.2147/IJN.S97476> <https://www.dovepress.com/targeted-polyethylene-glycol-gold-nanoparticles-for-the-treatment-of-p-peer-reviewed-article-IJN>.
- Torrissi L, Guglielmino S, Silipigni L, et al. Study of gold nanoparticles transport by M13-phages towards disease tissues as targeting procedure for radiotherapy applications. *Nano Res* 2018 (submitted for publication).
- NIST, X-Ray Mass Attenuation Coefficients, actual website 2018: <https://www.nist.gov/pml/x-ray-mass-attenuation-coefficients>.
- Ziegler J, SRIM, The Stopping and Range of Ions in the Matter, actual website 2018: <http://www.srim.org/>.
- SREM, The Stopping and Range of Electrons in the Matter, actual website 2018: <http://www.srim.org/SREM.htm>.
- Hidayat K, Chen GC, Zhang R, et al. Calcium intake and breast cancer risk: meta-analysis of prospective cohort studies. *Br J Nutr* 2016;116(1):158–66, <http://dx.doi.org/10.1017/S0007114516001768> <https://pdfs.semanticscholar.org/49af/9649debc7f28d0b-75e6654daa6aa7cfc8b28.pdf>.
- Beckett KR, Moriarity AK, Langer JM. Safe use of contrast media: what the radiologist needs to know. *Radiographics* 2015;35(6):1738–50, <http://dx.doi.org/10.1148/rg.2015150033> <https://www.ncbi.nlm.nih.gov/pubmed/26466182>.
- Gerweck LE, Kozin SV. Relative biological effectiveness of proton beams in clinical therapy. *Radiother Oncol* 1999;50(2):135–42 <https://www.ncbi.nlm.nih.gov/pubmed/10368035>.
- Thwaites DI. Bragg’s rule of stopping power additivity: a compilation and summary of results. *Radiat Res* 1983;95(3):495–518 <http://www.rrjournal.org/doi/abs/10.2307/3576096>.
- Hickey JW, Santos JL, Williford JM, Mao HQ. Control of polymeric nanoparticle size to improve therapeutic delivery. *J Control Release* 2015;219:536–47.
- Hainfeld JF, Slatkin DN, Smilowitz HM. The use of gold nanoparticles to enhance radiotherapy in mice. *Phys Med Biol* 2004;49:N309–15 <http://iopscience.iop.org/article/10.1088/0031-9155/49/18/N03/meta>.